
A combined crossed molecular beam and *ab initio* investigation of C₂ and C₃ elementary reactions with unsaturated hydrocarbons—pathways to hydrogen deficient hydrocarbon radicals in combustion flames

Ralf I. Kaiser,^{abc} Trung N. Le,^c Thanh L. Nguyen,^c Alexander M. Mebel,^c Nadia Balucani,^{cd} Yuan T. Lee,^c Frank Stahl,^{ef} Paul v. R. Schleyer^{ef} and Henry F. Schaefer III^f

^a Department of Chemistry, University of York, York, UK YO10 5DD

^b Department of Physics, Technical University Chemnitz-Zwickau, 09107 Chemnitz, Germany

^c Institute of Atomic and Molecular Sciences, Academia Sinica, 107 Taipei, Taiwan, ROC

^d Dipartimento di Chimica, Università di Perugia, 06123 Perugia, Italy

^e Institut für Organische Chemie der Universität Erlangen-Nürnberg, 91054 Erlangen, Germany

^f Center for Computational Quantum Chemistry, The University of Georgia, Athens, GA, 30602, USA

Received 1st March 2001

First published as an Advance Article on the web 26th September 2001

Crossed molecular beam experiments on dicarbon and tricarbon reactions with unsaturated hydrocarbons acetylene, methylacetylene, and ethylene were performed to investigate the dynamics of channels leading to hydrogen-deficient hydrocarbon radicals. In the light of the results of new *ab initio* calculations, the experimental data suggest that these reactions are governed by an initial addition of C₂/C₃ to the π molecular orbitals forming highly unsaturated cyclic structures. These intermediates are connected *via* various transition states and are suggested to ring open to chain isomers which decompose predominantly by displacement of atomic hydrogen, forming C₄H, C₅H, HCCCCCH₂, HCCCCCCH₃, H₂CCCCH and H₂CCCCCH. The C₂(¹ Σ_g^+) + C₂H₄ reaction has no entrance barrier and the channel leading to the H₂CCCCCH product is strongly exothermic. This is in strong contrast with the C₃(¹ Σ_g^+) + C₂H₄ reaction as this is characterized by a 26.4 kJ mol⁻¹ threshold to form a HCCCCCH₂ isomer. Analogous to the behavior with ethylene, preliminary results on the reactions of C₂ and C₃ with C₂H₂ and CH₃CCH showed the H-displacement channels of these systems to share many similarities such as the absence/presence of an entrance barrier and the reaction mechanism. The explicit identification of the C₂/C₃ *vs.* hydrogen displacement demonstrates that hydrogen-deficient hydrocarbon radicals can be formed easily in environments like those of combustion processes. Our work is a first step towards a systematic database of the intermediates and the reaction products which are involved in this important class of reactions. These findings should be included in future models of PAH and soot formation in combustion flames.

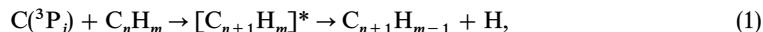
1. Introduction

Laboratory investigations on the reactions of small carbon molecules, dicarbon, C_2 and tricarbon, C_3 , with hydrocarbons are expected to elucidate possible formation pathways of hydrogen-deficient carbon chains and soot in a variety of terrestrial and astrophysical environments: high-temperature combustion flames, chemical vapor deposition (CVD) of diamond, outflow of asymptotic giant branch (AGB) carbon stars, comets, and interstellar clouds.¹ The spectral lines of dicarbon in its $^1\Sigma_g^+$ electronic ground state were first detected in comets more than a century ago² and in terrestrial hydrocarbon flames fifty years later.³ In the decades following it became clear that $C_2(X^1\Sigma_g^+)$ is ubiquitous in the interstellar medium.⁴ Transitions were observed towards warm carbons stars like IRC+10126,⁵ post AGB stars such as HD 56126,⁶ and towards the HII region W40 IRS. The tricarbon molecule was first assigned at the turn of the 19th century in comets⁷ prior to an identification in fuel flames,⁸ explosions,⁹ and during arc vaporization of carbon. Likewise, Hinkle *et al.* observed vibration-rotation transitions in the circumstellar shell of the carbon star IRC+10216, whereas Haffner and Meyer¹⁰ detected the infrared spectrum of $C_3(X^1\Sigma_g^+)$ in the translucent cloud HD147889.

Since the formation of small carbon clusters is thought to be strongly linked to the synthesis of polycyclic aromatic hydrocarbons (PAHs) and ultimately soot production in combustion flames,¹¹ laboratory studies are needed to assess the role of these species and to include them into the pertinent chemical models. Three kinds of laboratory results are crucial to describe the reactivity of small carbon clusters, namely the measurement of temperature-dependent rate constants, the identification of the reaction products, and an assignment of reaction intermediates. The kinetics of reactions involving the singlet ground state and the electronically excited triplet state of dicarbon have been extensively investigated¹² (recall that the electronically excited triplet state, a $^3\Pi_u$, lies only 718.32 cm^{-1} above the ground state $X^1\Sigma_g^+$). In these studies, the disappearance of C_2 in the two electronic states ($X^1\Sigma_g^+$ and $^3\Pi_u$) was followed; the reactions of $C_2(X^1\Sigma_g^+)$ were found to be quite fast (of the gas kinetic order when the molecular partner is an unsaturated hydrocarbon) whereas the $C_2(a^3\Pi_u)$ reactions were suggested to be systematically slower. Rate constants of C_3 reactions with several alkenes, alkynes, and allenes were found to be much smaller and seldom reached $10^{-12}\text{ cm}^3\text{ s}^{-1}$ range at room temperature.¹²

Despite these extensive kinetic investigation, information on the reaction products and intermediates involved is still lacking. In some cases, primary products and reaction mechanisms were postulated on the basis of the observed temperature dependence of the reactions. For instance, from the measured removal rate constants of both $C_2(X^1\Sigma_g^+)$ and $C_2(a^3\Pi_u)$ by ethylene and by halogen substituted ethylene, the favored approach was suggested to be an addition of the electrophilic C_2 (both singlet and triplet states) to the olefinic π bond. Nevertheless, $C_2(X^1\Sigma_g^+)$ reacts faster than $C_2(a^3\Pi_u)$ and is quite insensitive to halogen substitution. The reduced reactivity of $C_2(a^3\Pi_u)$ with the halogen-substituted ethylene was attributed to the hindrance of the bulky halogen atoms which hinders the approach to the π system. This implies that $C_2(X^1\Sigma_g^+)$ also reacts through alternative pathways. A few reactions of C_2 also were investigated at 77 and 10 K in the condensed phase and *ab initio* calculations were performed in order to help understand the reaction mechanism.¹³ Interestingly, the reaction products of the reaction of dicarbon with ethylene have been always assumed to be C_2H and C_2H_3 ($\Delta_rH = -75.5\text{ kJ mol}^{-1}$) or C_2H_2 and C_2H_2 ($\Delta_rH = -435.8\text{ kJ mol}^{-1}$). The formation of complex carbon chains such as $HCCCH_2$ and H , which actually is a strongly exothermic channel for both C_2 singlet and triplet states ($\Delta_rH = -156.3$ and $-165.5\text{ kJ mol}^{-1}$, respectively), has never been considered before. In contrast with the reaction of C_2 with C_2H_4 , the reaction C_3 with C_2H_4 was found to be slower, since the disappearance rate of C_3 resulted to be $<10^{-15}\text{ cm}^3\text{ s}^{-1}$ at $T = 294\text{ K}$ and an estimate of 27 kJ mol^{-1} for the activation energy was given. The reaction products were not identified in this reaction either.

A systematic study of the related reactions of atomic carbon, $C(^3P_j)$, with some unsaturated hydrocarbons (acetylene,¹⁴ methylacetylene,¹⁵ dimethylacetylene,¹⁶ propargyl,¹⁷ vinyl,²⁹ ethylene,¹⁸ propylene,¹⁹ buta-1,2-diene,²⁰ buta-1,3-diene,²¹ allene,²² and benzene²³) established that a C/H exchange channel is available in all cases. The reactions occur predominantly through the formation of a bound intermediate according to the general scheme:



Analogously, we expect that C_2 and C_3 can react with unsaturated hydrocarbons in a similar way through bound intermediates:



The occurrence of such reaction channels has been considered recently and investigated in crossed beam experiments with mass spectrometric detection.²⁴ The aim was to establish whether the formation of $C_{n+2}H_{m-1} + H$ and $C_{n+3}H_{m-1} + H$ is an open reactive channel or not. In order to elucidate the nature of the primary products, it is important to perform such experiments under single collision conditions. Thus in a binary reaction C_k ($k = 2, 3$) + $C_nH_m \rightarrow [C_{n+k}H_m]^* \rightarrow C_{n+k}H_{m-1} + H$, one carbon cluster C_k reacts with only one hydrocarbon molecule C_nH_m without collisional stabilization of the $[C_{n+k}H_m]^*$ complex(es) or successive reaction of the nascent reaction products. As implied from the general schemes (2) and (3), the primary products are highly hydrogen-deficient carbon clusters. These are extremely reactive and their spectroscopic properties are often unknown. Therefore, most of the combustion-relevant radicals are difficult to probe by optical detection methods. Resorting to a 'universal' detector is crucial in experiments when the nature itself of the product is obscure.

The crossed molecular beam technique with mass spectrometric detection has been established as a powerful technique to achieve these requirements and to observe radical product formation under well-characterized experimental conditions in the gas phase. Since investigations are performed at the molecular, microscopic level in a collision free environment—where it is possible to observe the consequences of a single reactive event—this approach provides a complete insight into the reaction mechanism as the nature of the primary reaction products can be inferred. When the products are polyatomic molecules, the crossed beam technique with mass spectrometric detection has proved to be essential in identifying the relevant reaction pathways.²⁵ In fact, when distinct structural isomers—molecules with the same chemical formula but different arrangements of atoms—might be formed, knowledge of chemical reaction dynamics is crucial in order to assign the isomers produced.

The first reactions we have investigated, involved C_2/C_3 and acetylene, C_2H_2 , ethylene, C_2H_4 , and methylacetylene, CH_3CCH . In order to assign the reaction mechanisms and products explicitly, the crossed molecular beam experiments were combined with high level *ab initio* calculations. The later yield structures and energies of possible intermediate collision complexes as well as reaction energies.²⁶ In this paper, we present experimental and theoretical results on the reaction of $C_2(X^1\Sigma_g^+, a^3\Pi_u)$ with C_2H_4 and report preliminary results on the reaction of $C_3(X^1\Sigma_g^+)$ with C_2H_4 . We also discuss other possible formation routes to the tricarbon molecule, *i.e.* the reaction of $C(^3P_j)$ with acetylene, and report on astrophysical and combustion implications of the reactions investigated.

2. Experimental and data analysis

All reactive scattering experiments were performed by using the 35" universal crossed molecular beam apparatus with mass spectrometric detection.²⁷ This machine consists of two source chambers fixed at 90° crossing angle, a stainless steel scattering chamber, and a ultra-high-vacuum (8×10^{-13} mbar) triply differentially pumped quadrupole mass spectrometric detector, *cf.* Fig. 1. The scattering chamber is evacuated by two oil free, magnetically suspended turbo pumps to a pressure in the range of 10^{-7} mbar. In the primary source, a pulsed supersonic beam of $C_2(X^1\Sigma_g^+/a^3\Pi_u)$ and $C_3(X^1\Sigma_g^+)$ is generated by laser ablation of a graphite rod at 266 nm and subsequent seeding of the liberated species in helium carrier gas.²⁸ Since dicarbon and tricarbon are simultaneously produced in the primary beam, in principle both species might react. However, this does not complicate the present experiments since at lower collision energies the reactions of $C_3(X^1\Sigma_g^+)$ cannot occur (they are either endothermic or have high entrance barriers, *cf.* Section 4). Consequently, the observed signals are attributable to C_2 reactions. On the other hand, when studying C_3 reactions, the H-displacement channels lead to products larger by 12 u than those

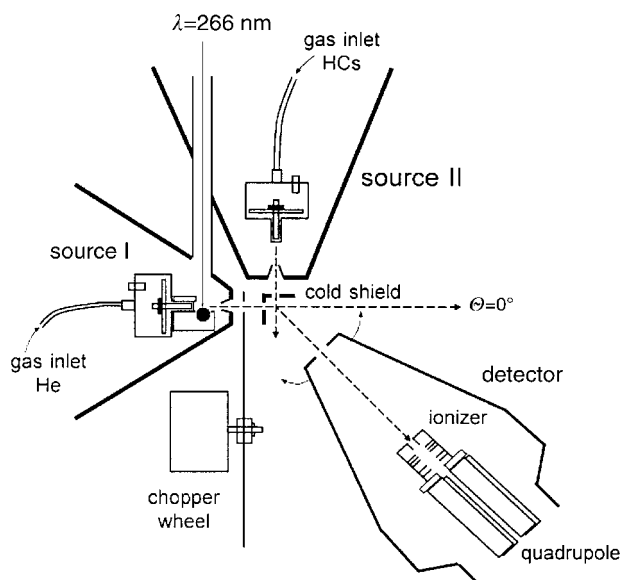


Fig. 1 Schematic top view of the 35" crossed molecular beams machine with source chambers, chopper wheel, and interaction region.

produced by C_2 reactions. Also, the relative contributions of C_2 vs. C_3 can be controlled by varying the laser output carefully between $20\text{--}95\text{ mJ pulse}^{-1}$, adjusting the focus diameter, and changing the delay time between the pulsed valve and the laser trigger. The primary beam passes through a skimmer into the main chamber. A four-slot chopper wheel is located after the skimmer and rotates at 240 Hz. It selects a $9\text{ }\mu\text{s}$ slice of well-defined velocity and speed ratio from the primary beam which reaches the interaction region. At this point, C_2 and C_3 collide at a right angle with the second pulsed beam of the unsaturated hydrocarbon at distinct collision energies selected between 18 and 120 kJ mol^{-1} .

The reactively scattered species are analyzed at different laboratory angles, θ , and at distinct mass-to-charge ratios, m/z , in the time-of-flight (TOF) mode. The intensity of an ion is recorded at a certain m/z vs. the flight time to yield a TOF spectrum at the laboratory angle θ ; the pulse of a photodiode attached to the chopper wheel is taken as a well-defined time zero for the experiments. We can integrate the TOF spectra taken at different laboratory angles and thus obtain the angular distribution of the product in the laboratory frame (LAB). The detector consists of a liquid-nitrogen-cooled electron impact ionizer followed by a quadrupole mass selector, and a Daly type ion detector; the ionizer is located in innermost part of a triply differentially pumped ultra-high-vacuum chamber. The whole detector unit can be rotated in the collision plane defined by the two intersecting beams. Despite the triply differential pumping set-up, molecules desorbing from wall surfaces lying on a straight line to the electron impact ionizer cannot be avoided. Their mean free path is in the order of 10^3 m compared to maximum detector dimensions of about 1 m. To reduce this background, a copper plate attached to a two stage closed cycle helium refrigerator is placed right before the collision center and cooled to 4.5 K. Thus the ionizer views a cooled surface which traps all the species with the exception of molecular hydrogen and helium.

For the physical interpretation of the reactive scattering data, it is necessary to transform the laboratory data into the center-of-mass (CM) system.⁹ Here, we employ a forward-convolution routine to fit the TOF spectra $N(\theta, t)$ at different laboratory angles and the LAB distribution. This procedure initially guesses the angular flux distribution, $T(\theta)$, and the translational energy flux distribution, $P(E_T)$, in the CM frame assuming mutual independence (θ is the scattering angle in the CM system measured with respect to the primary beam direction taken as $\theta = 0^\circ$ and E_T is the CM product translational energy). Then, TOF spectra and LAB distribution are calculated from these $T(\theta)$ and $P(E_T)$ by a routine which takes into account the velocity and angular spread of

both beams, the detector acceptance angle, and the ionizer length. Both $T(\theta)$ and $P(E_T)$ are refined until a satisfying fit of the experimental data is achieved.²⁹ The ultimate output data of our experiments is the generation of a product flux contour map which reports the differential cross section (the intensity of the reactively scattered products), $I(\theta,u) = P(u) \times T(\theta)$, as the intensity as a function of angle θ and product center-of-mass velocity u . The limiting circle is the maximum translational energy releases of the fragment if we assume that all the available energy channels only into the translational degrees of freedom of the products. The contour map serves as an image of the reaction and contains all the information of the scattering process.

3. The computational approach

All *ab initio* calculations on the singlet C_4H_4 , triplet C_4H_4 and singlet C_5H_4 PESs were carried out using the G2M(RCC,MP2) method,³⁰ which approximates the RCCSD(T)/6-311+G(3df,2p) energy.³¹ The geometries of the reactants, reaction intermediates, transition states, and products were optimized at the density functional B3LYP/6-311G** level.³² Vibrational frequencies calculated at this level were used for characterization of stationary points as minima and transition states, for zero-point energy (ZPE) corrections, and for RRKM calculations of reaction rate constants. The GAUSSIAN 94,³³ MOLPRO 98,³⁴ ACES-II,³⁵ and DALTON³⁶ *ab initio* program packages were employed.

Regarding the C_2/C_2H_2 system, geometries were optimized at UB3LYP/6-311+G** using the GAUSSIAN 98 program.³⁷ Each structure was confirmed as a minimum by frequency calculations at the same level and the unscaled UB3LYP/6-311+G** zero-point energies (ZPE) were used to correct the energies. Single point CCSD(T)/cc-pVTZ energies for the reactants and products were obtained using the ACES II program.³⁸

4. Results and discussion

4.1 The $C_2 + C_2H_4$ reaction

We have performed reactive scattering experiments at two different collision energies, $E_c = 14.7$ and 28.9 kJ mol^{-1} , by selecting different slices of the pulsed beams characterized by a peak velocity of $1200 \pm 8 \text{ m s}^{-1}$ and $1940 \pm 15 \text{ m s}^{-1}$ and a speed ratio of 9.0 ± 0.3 and 6.2 ± 0.2 , respectively. At both collision energies, signals were observed both at $m/z = 51$ ($C_4H_3^+$) and $m/z = 50$ ($C_4H_2^+$). However, since the TOF spectra at the two mass-to-charge ratios are superimposable, we conclude that under our experimental conditions the only product in this range of masses is C_4H_3 and that the ion $C_4H_2^+$ is actually formed in the ionizer by dissociative ionization. Fig. 2 displays selected TOF spectra recorded at the two collision energies, while Fig. 3 reports the laboratory angular distribution measured at the highest collision energy. The solid lines superimposed on the experimental distributions are the calculated curves when using the best-fit CM functions shown in Fig. 4 and 5. At these collision energies, tricarbon does not react with ethylene (*cf.* Section 4.2), and therefore cannot contribute to the observed signal. At all the collision energies investigated, the product CM angular distributions are symmetric with respect to $\theta = 90^\circ$; the best-fit angular distributions are reported for the lowest and the highest energy experiments in Fig. 5. The observed symmetry suggests that the reaction involves bound C_4H_4 intermediate(s) which has(have) a lifetime longer than its(their) rotational period. Interestingly, if we examine the product translational energy distributions reported in Fig. 4, we can see how at the lowest E_c the $P(E_T)$ peaks very close to zero translational energy, suggesting that the C_4H_4 complex dissociates to $C_4H_3 + H$ without exit barrier; at the higher collision energy a broad plateau from 0 to 45.3 kJ mol^{-1} is clearly visible. The dramatic change in shape might well imply the onset of a second reaction channel with the increase of the available energy. The tails of both distributions extend up to 159–201 and 151–210 kJ mol^{-1} , respectively.

The *ab initio* electronic structure calculations of the singlet potential energy surface (PES) show that $C_2(^1\Sigma_g^+)$ attacks the π -bond of C_2H_4 without an entrance barrier (Fig. 6), forming a three-member ring intermediate **il**. In contrast, the initial addition of $C_2(^3\Pi_u)$ to the π -system of ethylene on the triplet surface involves a barrier of less than 15.5 kJ mol^{-1} calculated at the G2M(RCC,MP2) level with MP2/6-311G** optimized geometry (this theoretical value probably is

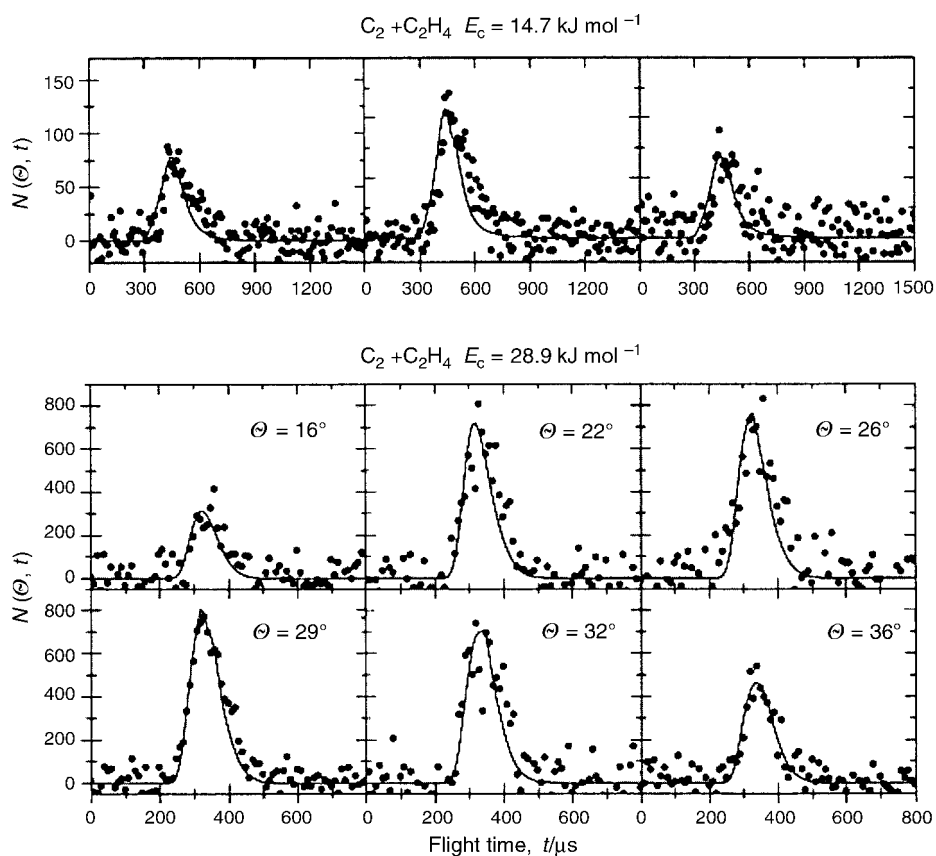


Fig. 2 Time-of-flight data of distinct laboratory angles of the reaction of dicarbon with ethylene to $HCCCCH_2 + H$ at a collision energy of 28.9 kJ mol^{-1} . The dots indicate the experimental data, the solid lines the calculated fit.

overestimated since an activation barrier $< 4 \text{ kJ mol}^{-1}$ has been estimated from kinetic measurements). This result is in contrast with earlier lower level HF/3-21G calculations which indicated that the addition of $C_2(^3\Pi_u)$ to ethylene occurs without a barrier. The singlet C_4H_4 PES reveals how the initially formed $i1$ complex (bound by 359 kJ mol^{-1} with respect to the reactants)

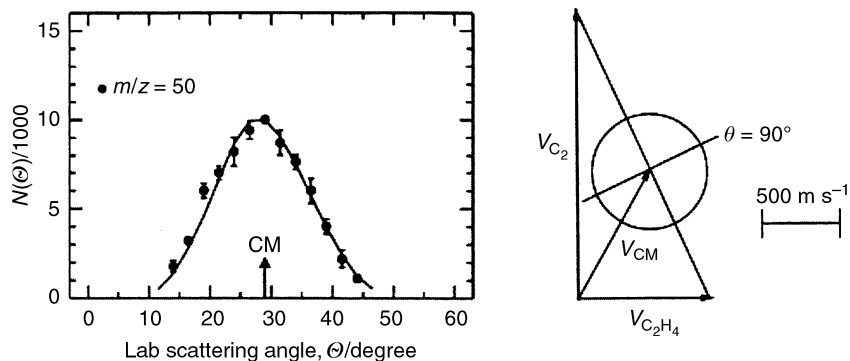


Fig. 3 Laboratory angular distribution of product channel at $m/z = 50$. Circles and 1σ error bars indicate experimental data, the solid lines the calculated distributions.

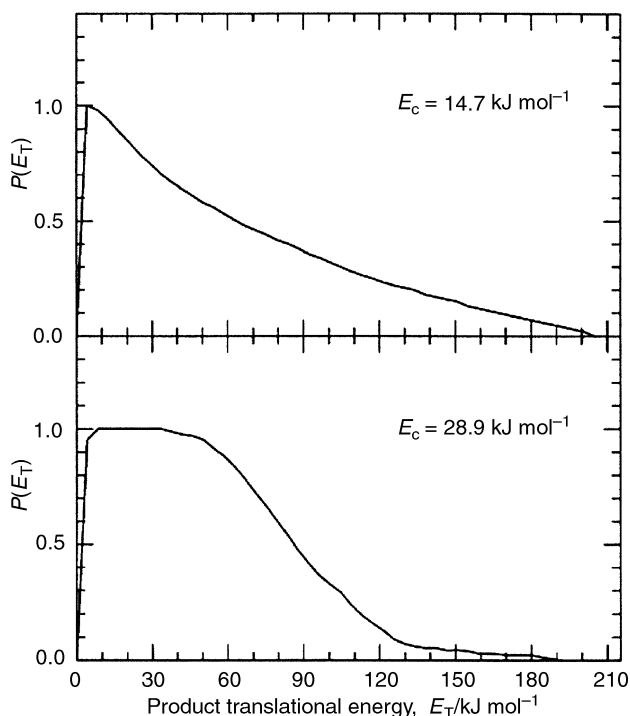


Fig. 4 Center-of-mass translational energy flux distributions at 14.7 kJ mol^{-1} (top) and 28.9 kJ mol^{-1} (bottom) of the reaction of C_2 with ethylene to C_4H_3 and atomic hydrogen.

might lose a hydrogen atom to **p4** or isomerizes to butatriene **i2**. The **i1** \rightarrow **i2** isomerization has a relatively low 59.5 kJ mol^{-1} barrier and is exothermic by 197 kJ mol^{-1} . Intrinsic reaction coordinate (IRC) calculations at the B3LYP/6-311G** level confirmed that the transition state actually connects **i1** and **i2**. Butatriene can eliminate a H atom to form the major reaction products, the HCCCCH_2 radical (**p1**) + H, without an exit barrier. The total reaction exothermicity to form **p1** + H from the reactants is calculated to be $156.3 \text{ kJ mol}^{-1}$.

The reaction of the C_2 triplet with ethylene is quite complex (Fig. 7). The addition of $\text{C}_2(^3\Pi_u)$ to the ethylene π -system forms intermediate **i1** bound by 127 kJ mol^{-1} with respect to the reactants. The initial intermediate can undergo ring closure to form a three-member ring species **i2**, which in turn would rearrange to a branched isomer **i4**, and then to another three-member cyclic intermediate, **i5**. Ring-opening of **i5** gives a linear triplet butatriene **i6** (391 kJ mol^{-1} below the reactants). **i6** loses a hydrogen atom to produce $n\text{-C}_4\text{H}_3$ **p1** with an overall exothermicity of 165 kJ mol^{-1} . The highest barrier on this pathway is located between **i2** and **i4** at 94 kJ mol^{-1} above **i2** and 33 kJ mol^{-1} below the reactants. A second route from **i1** to **i6** involves the four-member ring isomer **i3**, triplet cyclobutene. The ring closure from **i1** to **i3** is characterized by a barrier of 63 kJ mol^{-1} and the corresponding transition state is 63.7 kJ mol^{-1} lower in energy than the reactants. Subsequently, **i3** undergoes ring opening along the $\text{CH}_2\text{-CH}_2$ bond to yield **i6** with a barrier of 86 kJ mol^{-1} . Both pathways leading from **i1** to **i6** are expected to compete. Therefore, we conclude that like $\text{C}_2(^1\Sigma_g^+) + \text{C}_2\text{H}_4$, $n\text{-C}_4\text{H}_3$ (**p1**) is the major C_4H_3 product also for the $\text{C}_2(^3\Pi_u) + \text{C}_2\text{H}_4$ reaction.

The trend of our experimental data with increasing collision energy provides clear evidence of the involvement of a second reaction mechanism. Even though a spectroscopic characterization of the beam is needed in order to establish its exact ratio of triplet *vs.* singlet dicarbon, we expect that both the ground and the first electronically excited states of C_2 are present in the fast part of the beam because of the very small energy of the excited state. Therefore we can rationalize our observations in the light of the *ab initio* calculations of the singlet and triplet PES assuming

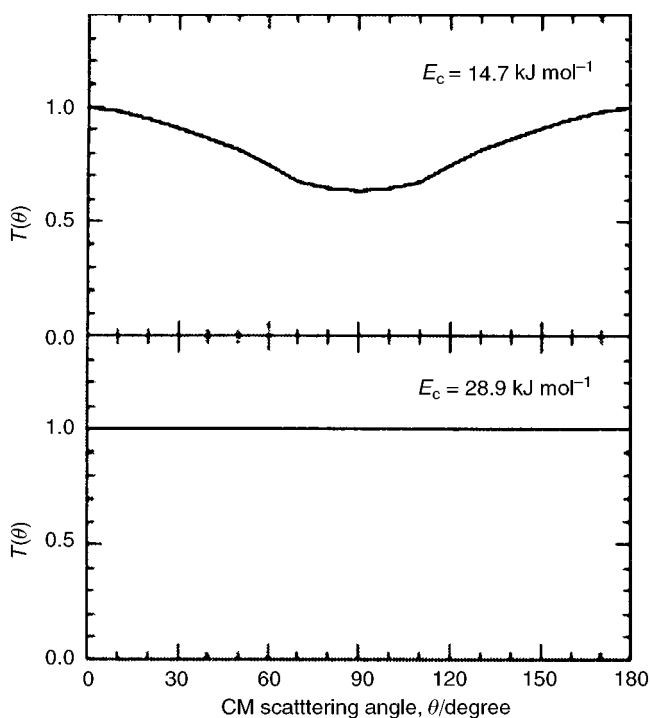


Fig. 5 Center-of-mass angular distributions at 14.7 kJ mol^{-1} (top) and 28.9 kJ mol^{-1} (bottom) of the reaction of C_2 with ethylene to C_4H_3 and atomic hydrogen.

that (i) at the lower collision energy we have a contribution to the recorded signal only from the $\text{C}_2(^1\Sigma_g^+)$ reaction and that (ii) an appreciable contribution from the triplet state reaction becomes evident only at the higher collision energy. In fact, although at this stage we do not know the exact barrier height for the triplet reaction, we expect an appreciable contribution from the triplet state reaction only when the collision energy is significantly larger than the reaction barrier. Hence, we can claim that the results of the low energy experiment are attributable for the most

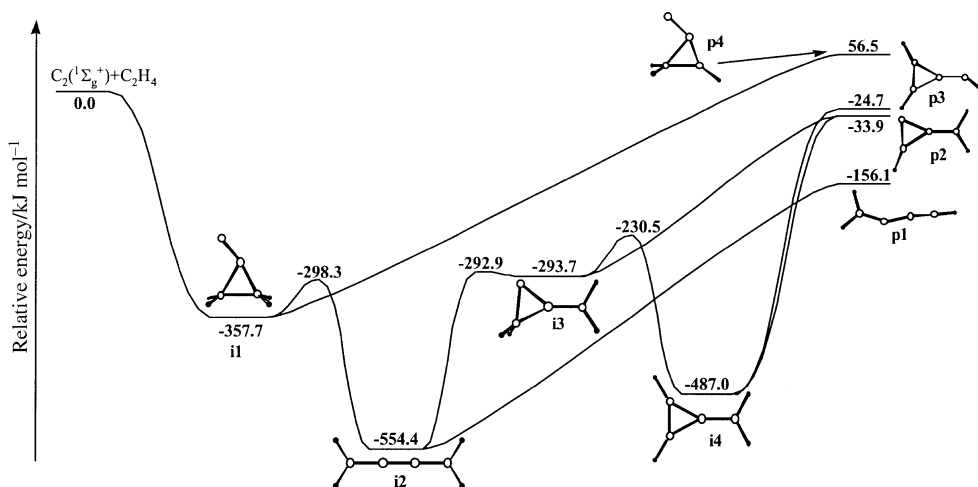


Fig. 6 Potential energy surface involved in the reaction of $\text{C}_2(\text{X } ^1\Sigma_g^+)$ with ethylene.

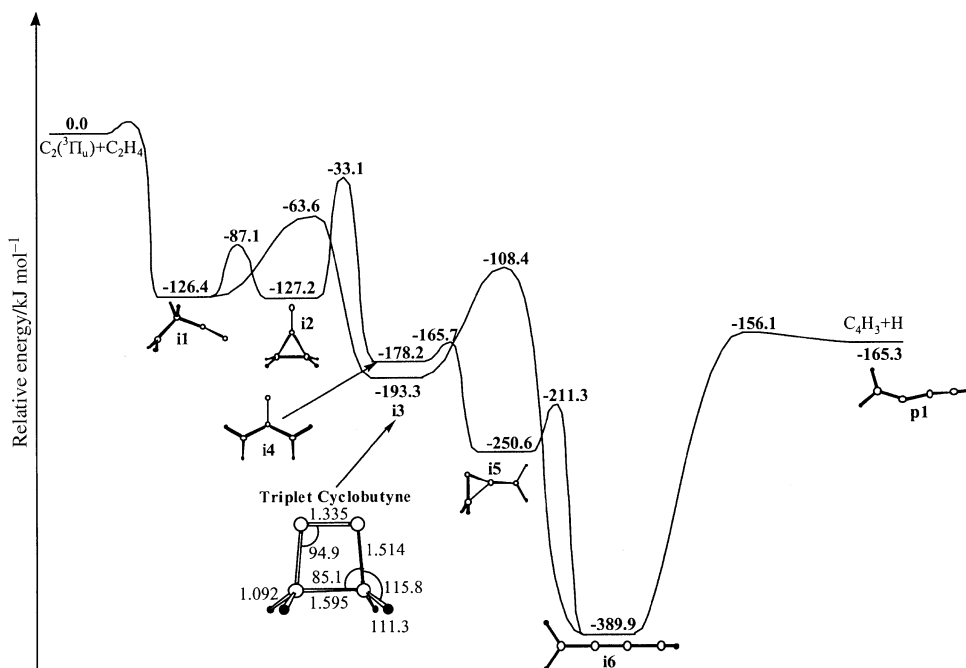


Fig. 7 Potential energy surface involved in the reaction of $C_2(a^3\Pi_u)$ with ethylene.

part to the $C_2(^1\Sigma_g^+)$ reaction. This assumption is supported strongly by our experimental data and *ab initio* calculations. As visible in Fig. 4, the $P(E_T)$ peaks at values of translational energy close to zero, thus mirroring the absence of any exit barrier as predicted by the calculations. Also, if we subtract the collision energy from the $P(E_T)$ energy maximum, we derive an exothermicity of 138–180 kJ mol^{-1} , which conforms with the *ab initio* value computed for this reaction channel. In addition, the decomposing butatriene complex resides in a deep potential energy well; this can well account for the observation of a backward–forward symmetric CM angular distribution. Also the assumption that the second mechanism is attributable to the $C_2(^3\Pi_u)$ reaction gains full support from the comparison of experimental results and theoretical calculations. That the second mechanism leading to C_4H_3 product has about the same reaction exothermicity as the first one, definitely rules out the occurrence of reaction channels leading to other isomers from the $C_2(^1\Sigma_g^+)$ reactions: the reaction enthalpies of the channels leading to **p2**, **p3** and **p4** are very different, see Fig. 6. Also, the peak of the translational energy distribution is quite broad and extends to 46 kJ mol^{-1} for the higher energy experiment, while in the lower energy experiment the peak is close to 0 kJ mol^{-1} . This change in the peak shape can be rationalized if the second channel has a (modest) exit barrier, as appears to be the case for the triplet reaction (see Fig. 7). In conclusion, the $C_2(^3\Pi_u)$ reaction on the triplet surface at high collision energy can well account for all the experimental facts.

4.2 The C_3 – C_2H_4 system

The experimental data analysis is still in progress and only some findings are presented. Interestingly, the C_3 –H exchange channel which forms products of $m/z = 63$ ($C_5H_3^+$) was found to occur, but was open only at collision energies larger than 40–42 kJ mol^{-1} in strong contrast to the $C_2 + C_2H_4$ reaction (which yields the products $C_4H_3 + H$ at lower collision energies). It is interesting to compare these results with the potential energy surface involved, *cf.* Fig. 8, as derived from our *ab initio* calculations. Similarly to the reaction of dicarbon with ethylene, the tricarbon molecule attacks the π -bond of the olefin to form a three-membered (**i1**) or a five-membered ring **i3** *via* addition of one or two terminal carbon atoms, respectively. Both structures

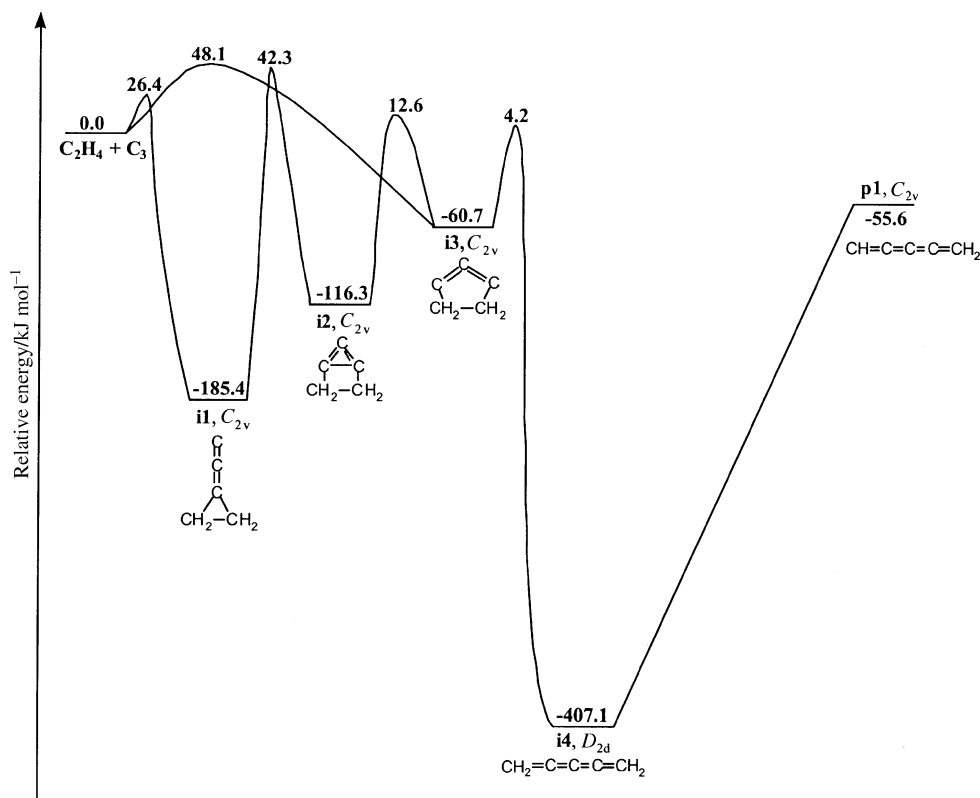


Fig. 8 Potential energy surface involved in the reaction of $C_3(X^1\Sigma_g^+)$ with ethylene.

are stabilized by 185.7 and 61 kJ mol^{-1} , respectively, and are connected through a bicyclic C_5H_4 isomer **i2**; the latter resides in a potential energy well of 116.5 kJ mol^{-1} . However, in strong contrast to the C_2 reaction, the C_3 addition involves entrance barriers of 26.4 and 48.2 kJ mol^{-1} to form **i1** and **i3**, respectively, as both processes are formally symmetry forbidden. This symmetry-imposed barrier was verified in previous bulk experiments which derived a value of 26.6 kJ mol^{-1} .¹² Interestingly, TOF and angular distributions measured at $m/z = 63$ and 62 are slightly different and that seems to imply that an H_2 elimination channel leading to C_5H_2 isomer(s) is open. A more accurate analysis of the raw data will shed light on this suggestion.

4.3 The $C_2-C_2H_2$, $C_3-C_2H_2$, $C_2-C_3H_4$ and $C_3-C_3H_4$ systems

The data analysis and electronic structure calculations of these reactions are still ongoing. We report only some observations here. Crossed beam experiments of C_2 with acetylene and with methylacetylene have resulted in the observation of the C_2 vs. H atom exchange pathway (forming C_4H ($m/z = 49$) and C_5H_3 ($m/z = 63$)) at collision energies as low as 8 kJ mol^{-1} and as high as 39 kJ mol^{-1} . A detailed study of the reaction with partially deuterated CD_3CCH showed that only the D atom is released (signal at $m/z = 65$, $C_5D_2H^+$); no H atom elimination at $m/z = 66$ ($C_5D_3^+$) could be detected. Both C_3 systems show reactive scattering signal of the C_3 vs. H atom exchange yielding C_5H ($m/z = 61$) and C_6H_3 ($m/z = 75$), only when the collision energy was higher than $80 \pm 9 \text{ kJ mol}^{-1}$ ($C_3-C_2H_2$) and $45 \pm 5 \text{ kJ mol}^{-1}$ ($C_3-C_3H_4$). Like the $C_2 + CH_3CCH$ system, the hydrogen atom was only emitted from the methyl group as in the $C_3 + CH_3CCH$ reaction. These findings, at this stage, suggest the possible reaction pathways sketched in Figs. 9 and 10, but these mechanisms are subject to further investigations.

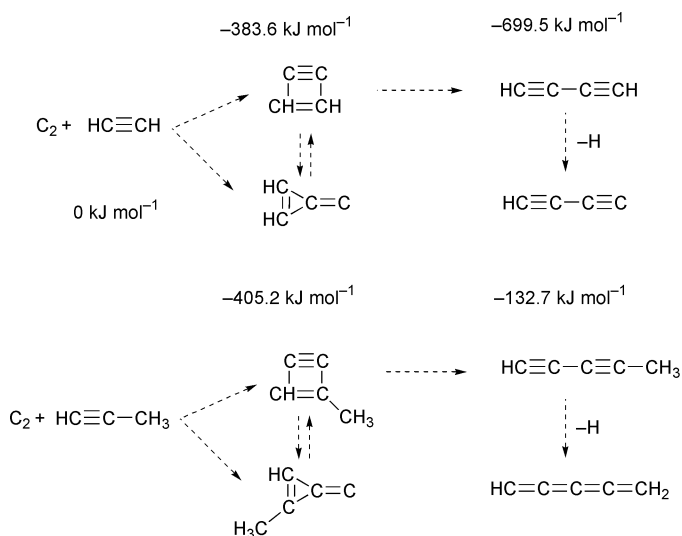


Fig. 9 Schematic pathways involved in the reaction of dicarbon with acetylene and methylacetylene. Energies for the C_2 - C_2H_2 system are given with respect to the separated reactants.

4.4 The $C(^3P_j)$ - C_2H_2 system

The reaction between ground state carbon atoms, $C(^3P_j)$, and acetylene, $C_2H_2(X^1\Sigma_g^+)$, was studied previously at three collision energies between 8.8 and 45.0 kJ mol^{-1} using the crossed molecular beams technique. Product angular distributions and time-of-flight spectra of C_3H at $m/z = 37$ and 36 were recorded. Reaction dynamics inferred from the experimental data and *ab initio* calculations on the triplet C_3H_2 and doublet C_3H potential energy surface suggest two microchannels initiated by addition of $C(^3P_j)$ either to one acetylenic carbon to form *s-trans*-propenediylidene or to two carbon atoms to yield triplet cyclopropenylidene *via* loose transition states located at their centrifugal barriers. Propenediylidene rotates around its B/C axis and a [2,3]-H-migration leads to propargylene. This is followed by C-H-bond cleavage *via* a symmetric

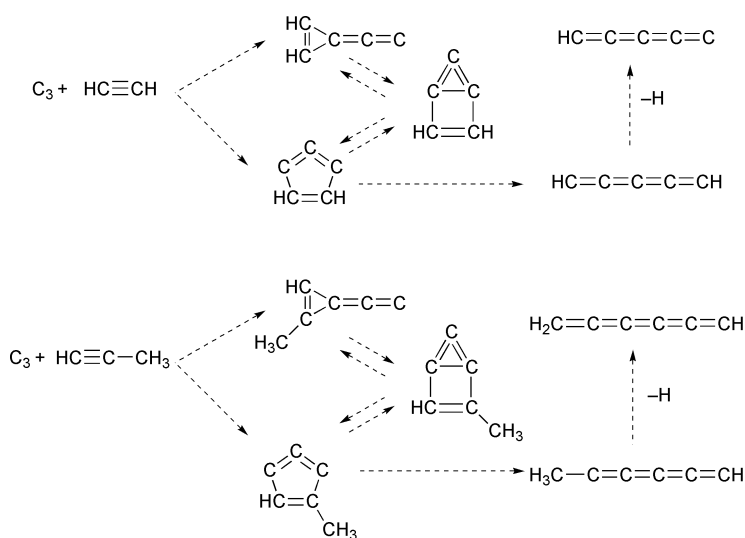


Fig. 10 Schematic pathways involved in the reaction of tricarbon with acetylene and methylacetylene.

exit transition state to give $\text{l-C}_3\text{H}(\text{X}^2\Pi)$ and H . Direct stripping dynamics contribute to the forward-scattered, second microchannel to yield $\text{c-C}_3\text{H}(\text{X}^2\text{B}_2)$ and H . This contribution is quenched with rising collision energy. TOFs of reactively scattered signal at $m/z = 36$ were found to be superimposable with those recorded at $m/z = 37$ suggesting that signal at $m/z = 36$ originates from cracking of $m/z = 37$ in the ionizer. However, the performance and signal to noise ratio of this experimental set-up was limited by the fact that diffusion pumps and oil lubricated roughing pumps were employed. Casavecchia *et al.*³⁹ suggested that C_3 might be an additional product of the $\text{C}(\text{}^3\text{P}_j) + \text{C}_2\text{H}_2$ reaction. However, their experiments employ continuous carbon beams which contain ground state and electronically excited $\text{C}(\text{}^1\text{D})$. Since multiple channel fits to one m/z ratio are not always ‘unique’, the need to reinvestigate the potential $\text{C}_3(\text{}^1\Sigma_g^+) + \text{H}_2(\text{}^1\Sigma_g^+)$ pathway with the improved, 35" crossed beams machine was stressed.²⁷

This experiment was repeated at a collision energy of 16.6 kJ mol^{-1} , under conditions where the beam contains only ground state carbon atoms. TOF spectra were recorded at $m/z = 37$ and $m/z = 36$ at angles between 12° and 72° with respect to the primary beam.⁴⁰ Fig. 11 shows the TOF recorded at the center-of-mass angle at 47° at $m/z = 36$; the data accumulation time was 120 min. Two components are clearly visible, *i.e.* a slow peak which arises from fragmentation of $m/z = 37$, and a fast contribution which could not be fit with the CM functions employed for the forward-convolution of the $m/z = 37$ data. The best fit CM translational energy distributions of the fast contribution is shown in Fig. 12, incorporating products of 36 and 2 u, *i.e.* the channel $\text{C}_3(\text{}^1\Sigma_g^+) + \text{H}_2(\text{}^1\Sigma_g^+)$, in the fitting routine. The TOFs were fit with a symmetric, slightly sideways peaking $T(\theta)$. Within the error limits, acceptable fits were achieved with intensity ratios $I(90^\circ)/I(0^\circ) = 1.3\text{--}1.1$; an isotropic distribution yields a slightly worse fit. These findings suggest that the decomposing complex is either long-lived or ‘symmetric’. Further, the $P(E_T)$ peaks between 70 and 100 kJ mol^{-1} indicating that the reaction involves a tight exit transition state. If we subtract the collision energy from the high energy cut-off of the $P(E_T)$ within the error limits, the reaction is found to be exothermic by $140\text{--}150 \text{ kJ mol}^{-1}$. These data are in good agreement with a reaction energy of $130\text{--}135 \text{ kJ mol}^{-1}$ calculated from thermodynamical data.⁴¹ The reaction from the triplet manifold to form $\text{C}_3(\text{}^1\Sigma_g^+)$ and molecular hydrogen is spin-forbidden, and intersystem crossing (ISC) from the singlet manifold is involved. A recent investigation of C_3H_2 isomers suggested that triplet propargylene, HCCCH , can indeed undergo ISC to the singlet surface,⁴² followed by loss of molecular hydrogen from singlet propargylene or—after isomerization—from vinylidencarbene *via* exit transition states well above the separated products.⁴³ This finding of a tight exit transition state correlates nicely with the translational energy distribution peaking well away from zero. Summarizing, we conclude that the $\text{C}_3(\text{}^1\Sigma_g^+) + \text{H}_2(\text{}^1\Sigma_g^+)$ pathway is open.

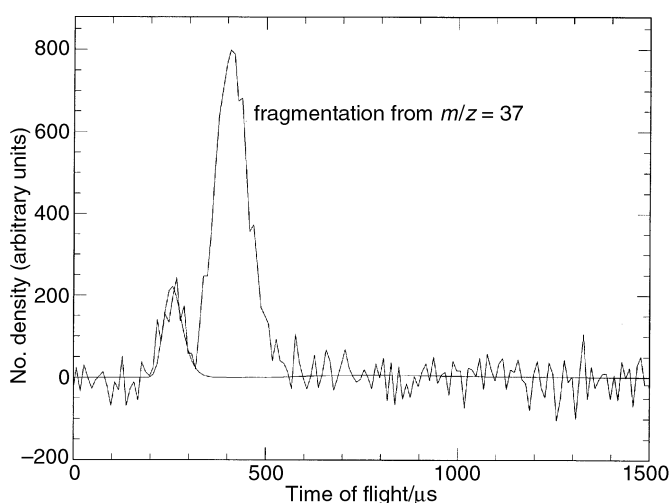


Fig. 11 Time-of-flight data at $m/z = 36$ of the reaction of atomic carbon with acetylene recorded at a laboratory angle of 47° . The smooth line represents the best fit.

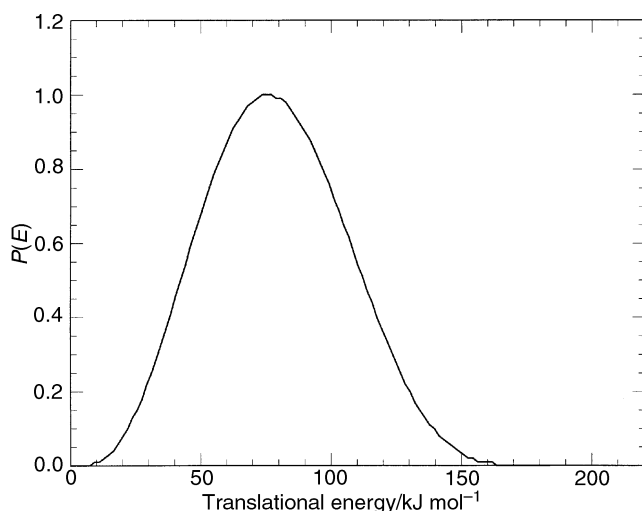


Fig. 12 Center-of-mass translational energy distribution of the reaction $\text{C}(^3\text{P}_j) + \text{C}_2\text{H}_2(^1\Sigma_g^+) \rightarrow \text{C}_3(^1\Sigma_g^+) + \text{H}_2(^1\Sigma_g^+)$.

This finding of an ISC to the singlet surface has far reaching consequences for the $\text{C}(^3\text{P}_j)\text{-C}_2\text{H}_2$ system as our previous interpretation focused solely on the triplet surface. Therefore, a more detailed interpretation of the experimental data including ISC is necessary. Further, this finding makes it interesting to investigate similar, substituted triplet propargylene systems, *cf.* Fig. 13. As triplet methylpropargylene and dimethylpropargylene were found to be the decomposing complexes in the reactions of atomic carbon with methylacetylene and dimethylacetylene, respectively, a possible ISC might be followed by CH_4 and C_2H_6 elimination *via* five-membered ring transition

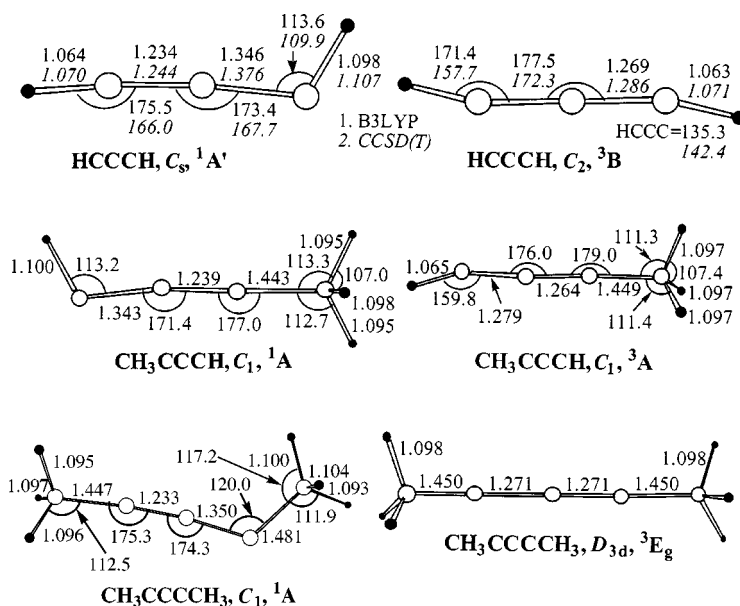


Fig. 13 Triplet (right) and singlet (left) structures of propargylene (top), methylpropargylene (middle) and dimethylpropargylene (bottom).

states from singlet methylpropargylene and dimethylpropargylene. Interestingly, all triplet propargylene structures were found to be lower in energy than the singlet species, and the singlet–triplet splitting was found to be 52.8 kJ mol^{-1} (propargylene), 33.5 kJ mol^{-1} (methylpropargylene), and 38.1 kJ mol^{-1} (dimethylpropargylene). The pathways of a potential methane and ethane elimination are subject to further investigations.

5 Conclusions

Our combined crossed molecular beam experiments and *ab initio* calculations on the reactions of dicarbon and tricarbon molecules with three unsaturated hydrocarbons, acetylene, methylacetylene, and ethylene, are governed by an initial addition of C_2/C_3 to the π bonds. Under single collision condition, highly unsaturated cyclic structures are formed. These intermediates are interconnected *via* various transition states and are suggested to ring open to HCCCCCH ($\text{C}_2 + \text{C}_2\text{H}_2$), HCCCCCH ($\text{C}_3 + \text{C}_2\text{H}_2$), HCCCCCH₃ ($\text{C}_2 + \text{CH}_3\text{CCH}$), HCCCCCH₃ ($\text{C}_3 + \text{CH}_3\text{CCH}$), H₂CCCCCH₂ ($\text{C}_2 + \text{C}_2\text{H}_4$) and H₂CCCCCH₂ ($\text{C}_3 + \text{C}_2\text{H}_4$). The chain isomers were found to decompose predominantly by atomic hydrogen loss yielding C_4H , C_5H , HCCCCCH₂, HCCCCCH₃, H₂CCCCCH and H₂CCCCCH. The role of possible cyclic reaction products and potential H₂ elimination pathways are currently under investigation. Our preliminary data suggest further that all reactions of $\text{C}_2(^1\Sigma_g^+)$ most likely have no entrance barriers and are exothermic. This is in strong contrast to bimolecular reactions of the tricarbon molecule $\text{C}_3(^1\Sigma_g^+)$ as these reactions have characteristic thresholds between 40 and 85 kJ mol^{-1} .

These findings have strong implications with respect to combustion processes. First, the explicit identification of the hydrogen replacement by C_2/C_3 demonstrates that hydrogen-deficient hydrocarbon molecules can be formed in combustion environments. We identified at least six distinct reaction products and more than 24 potential reaction intermediates. Although under our experimental single collision conditions the intermediates involved cannot be stabilized *via* a third body reaction, the conditions are more complex in actual combustion processes. Here, number densities are typically in the order of 10^{17} cm^{-3} at temperatures between 1000 and 2000 K, and ternary reactions might stabilize the reaction intermediates. The elevated temperatures open further reaction pathways which, like the elementary reactions of $\text{C}_3(^1\Sigma_g^+)$, either are endothermic and/or involve a significant entrance barrier. Although the full data analyses are still continuing, our investigations demonstrated the capability of reactions of small carbon molecules with unsaturated hydrocarbons to synthesize hydrogen-deficient molecules in combustion flames. This is a first step towards building a systematic database of intermediates and reaction products involved in this important reaction class. These should be included in future models of combustion flames as well as PAH and soot formation.

Although this Faraday Discussion focuses on combustion processes, we wish to briefly address the astrophysical implications of this research. In fact, more than once, combustion chemists and astrophysicists have employed similar reaction networks to explain the chemistry of these environments; multi-component models of carbon cluster growth and the correlation with PAH and soot formation are examples.⁴⁴ Several isomers of the carbon chain radicals with the general formula C_nH have been detected in the interstellar medium.⁴⁵ Therefore, our experimental and theoretical findings can help in explaining the formation of the C_4H and C_5H radicals as detected towards the cold molecular clouds TMC-1 and the carbon star IRC+10126, respectively. To our best knowledge, no ion–molecule reaction network can explain the formation of these isomers satisfactorily, and the crossed beam results present compelling evidence that neutral–neutral reactions might produce C_4H and C_5H *via* reactions of small carbon clusters with acetylene. While the average translation temperature of species in cold molecular clouds is typically 10 K, the temperatures rise up to 4000 K close to the photosphere of carbon stars. Based on these considerations, reactions of $\text{C}_3(^1\Sigma_g^+)$ are prohibited in interstellar dark clouds since the average translational energy cannot overcome the experimentally-determined entrance barriers and/or endothermicities. However, these elementary processes are open in the outflows of carbon stars because of the elevated temperature. In contrast, C_2 reactions were found to be exothermic and barrier-less and should occur even at temperatures as low as 10 K. Our preliminary data on the C_2/C_3 reactions with acetylene suggest that the alternating C_nH and C_mH ($n = \text{even}$, $m = \text{odd}$) abundance in interstellar environments might be a result of distinct chemical reactivity and exo-

thermicity; clearly, more experimental data—especially reactions of small carbon clusters with diacetylene and larger clusters with acetylene and diacetylene—are crucial to obtain more detailed, systematic correlations.

Acknowledgements

RIK is indebted to the Deutsche Forschungsgemeinschaft (DFG) for a Habilitation fellowship (IIC1-Ka1081/3-1). The experimental work was supported by Academia Sinica until September 2000. Hereafter, support from University of York, Department of Chemistry, is acknowledged. AMM thanks the National Science Council for support on the C₂-C₂H₄ and C₃-C₂H₄ calculations. FS greatly acknowledges a DAAD HSP III - Doktoranden fellowship (D/99/22963). Work in Erlangen was further supported by the DFG and the Fond der Chemischen Industrie. Work in Georgia was funded by the US Department of Energy. This work was performed within the International Astrophysics Network.

References

- 1 A. G. Gordon, *The Spectroscopy of Flames*, Wiley, New York, 1974; A. P. Baronavski and J. R. McDonald, *J. Chem. Phys.*, 1977, **66**, 3300; S. Green, *Annu. Rev. Phys. Chem.*, 1981, **32**, 103; D. C. Clary, *Annu. Rev. Phys. Chem.*, 1990, **41**, 61; S. R. Federman and D. L. Lambert, *Astrophys. J.*, 1988, **328**, 777; H. W. Kroto and K. McKay, *Nature*, 1988, **331**, 328.
- 2 M. R. Combi and U. Fink, *Astrophys. J.*, 1997, **484**, 879; K. S. K. Swamy, *Astrophys. J.*, 1997, **481**, 1004; P. Rousselot, C. Laffont, G. Moreels and J. Clairemidi, *Astron. Astrophys.*, 1998, **335**, 765.
- 3 A. P. Baronovski and J. R. McDonald, *J. Phys. Chem.*, 1977, **66**, 3300; A. G. Gaydon and H. G. Wolfhard, *Flames*, Chapman and Hall, New York, 1979; W. Weltner and R. J. van Zee, *Chem. Rev.*, 1989, **89**, 1713.
- 4 R. Gredel, *Astron. Astrophys.*, 1999, **351**, 657; I. A. Crawford, *Mon. Not. R. Astron. Soc.*, 1997, **290**, 41.
- 5 S. B. Yorke, *Astrophys. J.*, 1983, **88**, 1816.
- 6 I. A. Crawford and M. J. Barlow, *Mon. Not. R. Astron. Soc.*, 2000, **311**, 370.
- 7 W. Huggins, *Proc. R. Soc. London*, 1882, **33**, 1.
- 8 A. E. Douglas, *Astrophys. J.*, 1951, **114**, 446; H. H. Nelson, H. Helvajian, L. Pasternack and J. R. McDonald, *Chem. Phys.*, 1982, **73**, 431.
- 9 R. G. Norrish, G. Porter and B. A. Thrush, *Proc. R. Soc. London, Ser. A*, 1953, **216**, 165.
- 10 L. M. Haffner and D. M. Meyer, *Astrophys. J.*, 1995, **453**, 450.
- 11 Y. T. Lin, R. K. Mishra and S. L. Lee, *J. Phys. Chem. B*, 1999, **103**, 3151; N. Balucani *et al.*, *J. Chem. Phys.*, 1991, **94**, 8611; M. Alagia *et al.*, *J. Chem. Soc., Faraday Trans.*, 1995, **91**, 575; M. Alagia *et al.*, *Faraday Discuss.*, 1999, **113**, 133.
- 12 W. M. Pitts, L. Pasternack and J. R. McDonald, *Chem. Phys.*, 1982, **68**, 417; L. Pasternack, W. M. Pitts and J. R. McDonald, *Chem. Phys.*, 1981, **57**, 19; V. M. Donnelly and L. Pasternack, *Chem. Phys.*, 1979, **39**, 427; L. Pasternack and J. R. McDonald, *Chem. Phys.*, 1979, **43**, 173; H. Reisler, M. Mangir and C. Wittig, *J. Chem. Phys.*, 1979, **71**, 2109; K. H. Becker, B. Donner, H. Geiger, F. Schmidt and P. Wiesen, *Z. Phys. Chem.*, 2000, **214**, 503; M. Martin, *J. Photochem. Photobiol. A*, 1992, **66**, 263.
- 13 P. S. Skell, L. M. Jackman, S. Ahmed, M. L. McKee and P. B. Shevlin, *J. Am. Chem. Soc.*, 1989, **111**, 4422; G. H. Jeong, K. J. Klabunde, O. G. Pan, G. C. Paul and P. B. Shevlin, *J. Am. Chem. Soc.*, 1989, **111**, 8784.
- 14 R. I. Kaiser, C. Ochsenfeld, M. Head-Gordon, Y. T. Lee and A. G. Suits, *Science*, 1996, **274**, 1508.
- 15 R. I. Kaiser, D. Stranges, Y. T. Lee and A. G. Suits, *J. Chem. Phys.*, 1996, **105**, 8721.
- 16 L. C. L. Huang, H. Y. Lee, A. M. Mebel, S. H. Lin, Y. T. Lee and R. I. Kaiser, *J. Chem. Phys.*, 2000, **113**, 9637.
- 17 R. I. Kaiser, W. Sun, A. G. Suits and Y. T. Lee, *J. Chem. Phys.*, 1997, **107**, 8713.
- 18 R. I. Kaiser, Y. T. Lee and A. G. Suits, *J. Chem. Phys.*, 1996, **105**, 8705.
- 19 R. I. Kaiser, D. Stranges, H. M. Bevssek, Y. T. Lee and A. G. Suits, *J. Chem. Phys.*, 1997, **106**, 4945.
- 20 N. Balucani, A. M. Mebel, H. Y. Lee, Y. T. Lee and R. I. Kaiser, *J. Chem. Phys.*, 2001, in press.
- 21 I. Hahndorf, H. Y. Lee, A. M. Mebel, S. H. Lin, Y. T. Lee and R. I. Kaiser, *J. Chem. Phys.*, 2000, **113**, 9622.
- 22 R. I. Kaiser, A. M. Mebel, A. H. H. Chang, S. H. Lin and Y. T. Lee, *J. Chem. Phys.*, 1999, **110**, 10300.
- 23 R. I. Kaiser *et al.*, *J. Chem. Phys.*, 1999, **110**, 6091.
- 24 R. I. Kaiser *et al.*, in *Astrochemistry—From Molecular Clouds to Planetary Systems*, ed. Y. C. Minh and E. F. van Dishoek, Associated Scientific Publishers, San Francisco, 2000, p. 251.
- 25 P. Casavecchia, *Rep. Progr. Phys.*, 2000, **63**, 355; P. Casavecchia, N. Balucani and G. Volpi, *Annu. Rev. Phys. Chem.*, 1999, **50**, 347.
- 26 C. Ochsenfeld, R. I. Kaiser, A. G. Suits, Y. T. Lee and M. Head-Gordon, *J. Chem. Phys.*, 1997, **106**, 4141.
- 27 N. Balucani, O. Asvany, Y. Osamura, L. C. L. Huang, Y. T. Lee and R. I. Kaiser, *Plan. Space Sci.*, 2000, **48**, 447.

- 28 R. I. Kaiser and A. G. Suits, *Rev. Sci. Instrum.*, 1995, **66**, 5405.
- 29 R. I. Kaiser, C. Ochsenfeld, D. Stranges, M. Head-Gordon and Y. T. Lee, *Faraday Discuss.*, 1998, **109**, 183.
- 30 A. M. Mebel, K. Morokuma and M. C. Lin, *J. Chem. Phys.*, 1995, **103**, 7414.
- 31 G. D. Purvis and R. J. Bartlett, *J. Chem. Phys.*, 1982, **76**, 1910; C. Hampel, K. A. Peterson and H. J. Werner, *Chem. Phys. Lett.*, 1992, **190**, 1; P. J. Knowles, C. Hampel and H. J. Werner, *J. Chem. Phys.*, 1994, **99**, 5219; M. J. O. Deegan and P. J. Knowles, *Chem. Phys. Lett.*, 1994, **227**, 321.
- 32 A. D. Becke, *J. Chem. Phys.*, 1993, **98**, 5648; C. Lee, W. Yang and R. G. Parr, *Phys. Rev. B*, 1988, **37**, 785.
- 33 M. J. Frisch *et al.*, *GAUSSIAN 94, Revision E.2*, Gaussian, Inc., Pittsburgh, PA, 1995.
- 34 *MOLPRO* is a package of *ab initio* programs written by H.-J. Werner and P. J. Knowles, with contributions from J. Almlöf, R. D. Amos, M. J. O. Deegan, S. T. Elbert, C. Hampel, W. Meyer, K. Peterson, R. Pitzer, A. J. Stone, P. R. Taylor and R. Lindh.
- 35 J. F. Stanton, J. Gauss, J. D. Watts, W. J. Lauderdale and R. J. Bartlett, *ACES-II*, University of Florida, Gainesville, FL.
- 36 T. Helgaker *et al.*, *DALTON, an ab initio electronic structure program, Release 1.0*, 1997.
- 37 M. J. Frisch *et al.*, *GAUSSIAN 98, Revision A.7*, Pittsburgh, PA, 1999.
- 38 J. F. Stanton, J. Gauss, J. D. Watts, M. Nooijen, N. Oliphant, S. A. Perera, P. G. Szalay and R. J. Bartlett, “*ACES II*”, Gainesville, FL, 1995.
- 39 P. Casavecchia, N. Balucani, L. Cartechini, G. Capozza, A. Bergeat and G. G. Volpi, *Faraday Discuss.*, 2001, **119**, (DOI: 10.1039/b102634h).
- 40 TOF close to the carbon beam showed a significant background from elastically scattered C_3 . We redid the $C(^3P) + C_2H_4$ reaction as well at a similar collision energy at 18 kJ mol^{-1} , but in this case no H_2 elimination pathway was observed experimentally.
- 41 *Handbook of Chemistry and Physics*, CRC Press, Boca Raton, 1998.
- 42 A. M. Mebel, W. M. Jackson, A. H. H. Chang and S. H. Lin, *J. Am. Chem. Soc.*, 1998, **120**, 5741.
- 43 R. I. Kaiser, A. M. Mebel and Y. T. Lee, *J. Chem. Phys.*, 2001, **114**, 231.
- 44 G. Pascoli and A. Polleux, *Astron. Astrophys.*, 2000, **359**, 799.
- 45 M. Ohishi and N. Kaifu, *Faraday Discuss.*, 1998, **109**, 205; M. Guelin, S. Green and P. Thaddeus, *Astrophys. J.*, 1978, **224**, L27; M. Cernicharo, C. Kahane, J. Gomez-Gonzalez and M. Guelin, *Astron. Astrophys.*, 1986, **164**, L1; C. M. Walmsley, P. R. Jewell, L. E. Snyder and G. Winnewisser, *Astron. Astrophys.*, 1984, **134**, L11; J. Cernicharo, M. Guelin, K. M. Menten and C. M. Walmsley, *Astron. Astrophys.*, 1987, **181**, L1; J. Guelin *et al.*, *Astron. Astrophys.*, 1997, **317**, L1; J. Cernicharo and M. Guelin, *Astron. Astrophys.*, 1996, **309**, L27; C. A. Gottlieb, M. C. McCarthy, K. J. Travers and P. J. Thaddeus, *Chem. Phys.*, 1998, **109**, 5433; T. J. Millar and E. Herbst, *Astron. Astrophys.*, 1994, **288**, 561.